

Student :: Jesse Dietderich Date :: April 19, 2010 Advisor :: Dr. Richard J. Walker

Class :: Geology 394

ABSTRACT

My senior thesis project examines the abundances of highly siderophile elements (HSE) present in group IIAB iron meteorites. The term siderophile derives from the Greek "sideros" (iron) and "philein" (to love), which means these HSE have a strong affinity for metallic iron. A model of fractional crystallization was developed to account for variations in these trace element concentrations. I measured the concentrations of the following suite of HSE; Re, Os, Ir, Ru, Pt, and Pd. After digestion of the iron meteorite, Os was separated by carbon tetrachloride solvent extraction, and purified via microdistillation. The rest of the elements were purified by the use of anion exchange chromatography. Mass spectrometry coupled with isotope dilution was used to precisely determine the concentrations of the six elements. Starting with a prior model for fractional crystallization that considered Re-Os + Pt abundances, I used it to fit the newly acquired data and modified the model to accommodate varying initial concentrations of S, P, and the suite of HSE. My sample suite spanned the full range of the IIAB iron's Ni content, and were modeled to a varying crystallization path, but the modeling of Pd resulted in an unsatisfactory fit.

1. INTRODUCTION

The Earth is a differentiated body where-by much of the iron has collected as metal in the core of the planet. The core, however, is inaccessible in terms of obtaining a sample for laboratory testing. This inability to obtain samples from such great depths is one reason why we study the differentiated cores of asteroids. The study of asteroids also provides us with information about processes that occurred in the early solar system. Fortunately, there have been

many samples of space debris delivered to our doorstep, some in the form of iron meteorites. Some iron meteorites are the remains of iron cores that segregated inside the bodies of asteroids. The asteroids have since broken up, and the resulting pieces have fallen to Earth. After determination of Fe, Ni, Ga, and Ge compositions, iron meteorites are grouped. Meteorites within the same "group" are believed to come from the same parent body. Genetically related (from the same body) irons provide us with the information to enable us to construct models for core formation and crystallization. The samples being studied for this project are group IIAB iron meteorites. The IIAB group has the second largest number of identified samples, and has the lowest nickel content of any of the major iron meteorite groups (Cook et al. 2004)(see Figure 1).

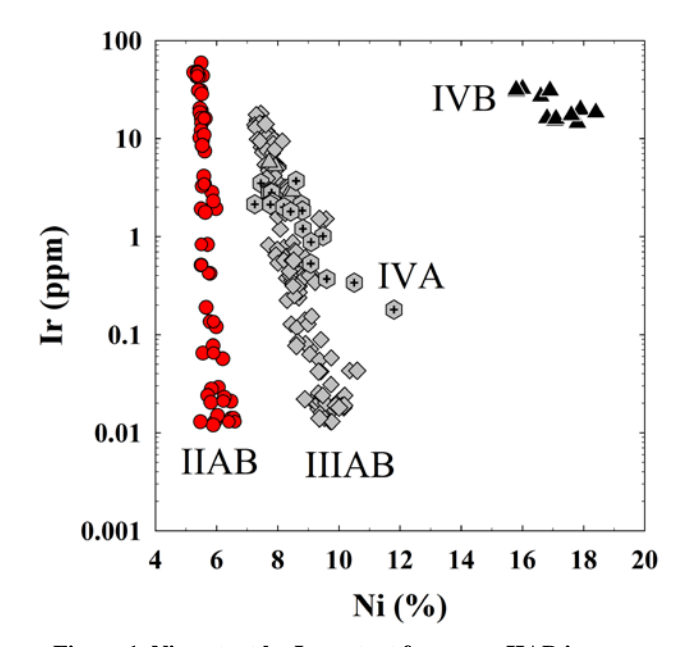


Figure 1. Ni content by Ir content for group IIAB irons (Walker et al. 2008)

This project focuses on the high temperature geochemistry of the IIAB core. More specifically, we are interested in the way that highly siderophile elements (HSE) behave during crystallization of the core. The HSE's attraction to iron causes a preference for HSE to become incorporated in metal during the formation of the core. There has been a great deal of work done on the group IIAB iron meteorites already. For example, Cook et al. (2004) studied both the isotopic and elemental systematics of Re, Os, and Pt in IIAB irons. Here the focus is exclusively on the abundances of the HSE. To obtain a more complete set of data than Cook et al. (2004), this thesis project includes analysis of Ru, Ir, and Pd, as well as, the previously measured and modeled Re, Os, and Pt. This project utilized the previous models of fractional crystallization of Cook et al. (2004) as a starting point, but required modification to accommodate the three additional trace elements.

The objective was to generate a model for the fractional crystallization of the core of the asteroid from which the group IIAB iron meteorite originated, using the HSE. This task has been accomplished by collecting trace element abundance data on the selected HSE suite and using those data to construct a model. My initial hypothesis was that only five of the HSE could be made to fit a single model. The projected rogue HSE was Pd, due to its initial incompatibility at the start of core formation. The null hypothesis for the project was that all six HSE would conform to an established model without the need of modification.

The data obtained helps future work on the group IIAB iron meteorites, regardless of a fully functional model. Completion of a working model for the fractional crystallization of the group IIAB iron meteorites furthers the understanding of asteroidal core formation.

2. ANALYTICAL METHODS

The bulk concentration data were obtained via isotope dilution coupled with mass spectrometry for each of the HSE. The IIAB samples were initially inventoried and organized by Ni content, in order to select samples that span the known compositional range of the group. After selecting the first batch of samples, I proceeded to prepare eight samples for digestion. Oxidation was removed by using a carborundum sanding block. Then the samples were bathed in an ultrasonic ethanol bath to remove any residue from abrading. An electronic balance that measured to µg precision was used to determine the sample weight. The amount of spike needed for each sample was calculated using Os concentration data from published studies (Cook et al. 2004). Spikes are isotopically modified solutions of a given element, with precisely and accurately determined concentration. An appropriate amount of spike was then combined with the sample and an acid mixture of 5.05 mL concentrated HNO3 and 2.8 mL of concentrated HCl. The samples were then sealed in Pyrex Carius tubes. I placed the tubes in an oven set to 240°C for a 24-hour period in order to dissolve the meteorites and oxidize Os to its highest valence state. After removal from the oven, the samples were packed in ice to prevent Os evaporation. The Carius tubes were broken open and the contents transferred to centrifuge tubes for Os extraction.

The next step required each sample to be mixed with carbon tetrachloride and shaken to separate the Os from the iron matrix and other HSE. Then I extracted the denser CCl₄ via a disposable pipette, and deposited it in a Teflon vessel containing HBr. This process is a form of

solvent extraction and done multiple times to withdraw the maximum amount of Os. The remaining HSE were left in the acid in the centrifuge tubes until the Os purification process was complete. The extracted Os was further purified by microdistillation by re-oxidizing the sample with CrO₃ allowing the Os to transfer to a HBr droplet. The microdistillation yielded extremely pure Os form that can be run on the thermal ionization mass spectroscopy (TIMS).

The acid solution containing the remaining five HSE (Re, Ir, Ru, Pt and Pd) were placed in the Teflon used for the Os. After removing the acid via evaporation, the residue is processed through anion exchange columns to separate out the HSE into the following three groups; Re-Ru, Pt-Ir, and Pd. With all of the elements purified, they were then ready for analysis.

The next step was to use the TIMS to measure and calculate the Os concentrations via isotope dilution. This requires depositing the purified Os samples onto platinum filaments and loading the filaments into the TIMS. Prior to running the analysis, each sample needs to have its signal adjusted, by fine-tuning the current passing through the different plates in the source, in order to provide better detection while collecting the data. At the end of the analysis the TIMS prints out a final calculated concentration and uncertainty for that particular measurement. The TIMS was also used to analyze Re concentrations in the second batch of meteorite samples during a period while the ICP-MS was unavailable for use. These data were compared with data ultimately obtained from the ICP-MS but were not used when compiling the final data set.

The ICP-MS was used in a similar fashion to the TIMS, but rather than filaments, the sample is dissolved and converted into an aerosol using argon gas. The sample is injected into the plasma to be ionized. The ICP-MS uses the same isotope dilution method to determine the concentrations of the Re, Ir, Ru, Pt, and Pd. Both the TIMS and the ICP-MS provided the standard deviation of the mean for each of the ratio measurements. The first batch of samples were analyzed on the Nu-Plasma, while the second batch of samples were run on the Element 2 due to time constraints.

The mass spectrometers provide isotopic ratios, which were used when calculating the concentrations by isotope dilution. For example, in the case of the Os analysis, the TIMS provided ¹⁹⁰Os/¹⁹²Os ratio, which was necessary in order to solve the isotope dilution equation for Os (see equation 1). To determine the number of atoms present in a sample, you need to know the sample's weight, atomic weight, and atomic fractionation, as well as the spike's weight, atomic weight, atomic fractionation, and concentration. The required measurements are the weight of the sample, the weight of the spike, the concentration of the spike and the measured ¹⁹⁰Os/ ¹⁹²Os ratio. The rest of the calculation has known variables such as atomic weights and atomic percentages. The final step, to algebraically solve for the only unknown variable, which is the quantity of the element from the sample.

Equation 1. The isotope dilution equation used for Os.

$$\frac{190}{192} = \frac{\left(\# \ atoms \ of \ ^{190}Os \ in \ sample\right) + \ (\# \ atoms \ of \ ^{190}Os \ in \ spike)}{\left(\# \ atoms \ of \ ^{192}Os \ in \ sample\right) + \ (\# \ atoms \ of \ ^{192}Os \ in \ spike)} = \frac{(A) + (B)}{(C) + (D)}$$

Continuation of Equation 1. Each of the four parts on the right hand side of the equation are broken up into equations A, B, C & D, which further describe what was done.

$$(A) = \frac{(quantity \ of \ sample \ Os)(atomic \ \%^{190}Os \ sample)}{(atomic \ weight \ of \ sample \ Os)}$$

$$(B) = \frac{(quantity \ of \ spike \ Os)(atomic \ \%^{190}Os \ spike)}{(atomic \ weight \ of \ spike \ Os)}$$

$$(C) = \frac{(quantity \ of \ sample \ Os)(atomic \ \%^{192}Os \ sample)}{(atomic \ weight \ of \ sample \ Os)}$$

$$(D) = \frac{(quantity \ of \ spike \ Os)(atomic \ \%^{192}Os \ spike)}{(atomic \ weight \ of \ spike \ Os)}$$

There are several analytical uncertainties present in this project and they are easy to identify and calculate. One uncertainty comes from the weighing of both the iron meteorite samples and of the spikes. Two separate balances were used for weighing; the Mettler AT21 was used to weigh the samples and the Mettler AE240 was used to weigh the spikes. I measured the weight of a spare IIAB iron meteorite three times on three separate days on both the AT21 and AE240 balances. The results from weighing the spare meteorite gave me a relative standard deviation of $\pm 0.0034\%$ for the AT21 and $\pm 0.012\%$ for the AE240. The "Blanks" are contributions from chemical processing and lack any HSE from any iron meteorite samples. The mass spectrometric analytical uncertainties ranged from a low 0.1% for Os ratios achieved with the TIMS, to 0.2% for the Nu-Plasma ratios, and 0.5% for the ratios on the Element 2 (except for Pd that was 0.7%). Error magnification was then empirically determined by adjusting the isotope ratios by 1% and calculating the effect the adjustment had on the calculated abundances.

Another uncertainty in this project is not an analytical uncertainty, but is due to sample heterogeneity. I made it a point to scrutinize the duplicates I ran, and compare my data with previously acquired IIAB iron data. The results of four sets are shown in figure 2a-d. Reproducibility was determined initially to be 3% due to the differences in concentrations between the two Filomena samples, while the Santa Luzia samples in the second batch were 50% different for Pd. The existence of a Widmanstätten pattern in the iron meteorites indicates the partitioning of the Ni alloys kamacite and taenite. It is understandable that the dissolved iron meteorite samples are affected by this partitioning in the group IIAB iron meteorites. This uncertainty overrides all the other lesser uncertainties by a significant margin for the samples with high concentrations of Ir, but the analytical uncertainty is still dominant for the samples with low Ir abundances.

The total uncertainties were a combination of both the analytical uncertainties and those created by heterogeneity. I listed the total uncertainty values along with the concentration data in the final data table.

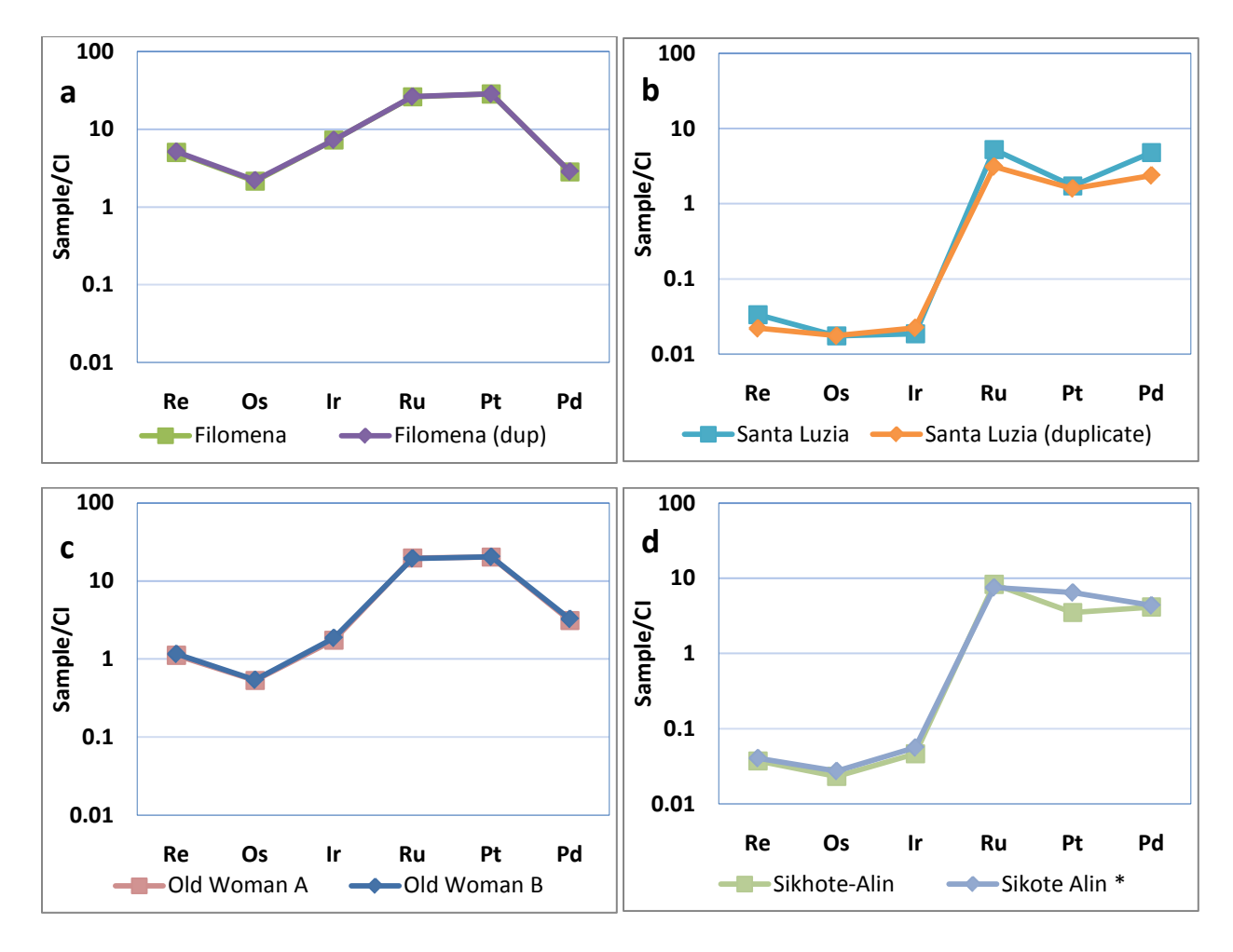


Figure 2. (a-d) Showing CI chondrite normalized abundances of duplicate analyses for (a) Filomena, (b) Santa Luzia, and (c) Old Woman. While the (d) Sikhote-Alin shows the comparison between my analysis and unpublished IGL data (marked with *).

3. RESULTSAll data are reported in Table 1 and then normalized to chondritic values (see figure 3).

Sample	Wt (g)	Ni (%)	Re (ppb)	±(%)	Os (ppb)	±(%)	Ir (ppb)	±(%)	Ru (ppb)	±(%)	Pt (ppb)	±(%)	Pd (ppb)	±(%)
Negrillos	0.05321	5.25	4623	0.75%	64460	1.16%	44520	1.26%	28100	0.64%	35100	0.75%	1454	1.07%
Bennett County	0.04337	5.4	4340	0.68%	56840	0.95%	42800	1.10%	27940	0.61%	35000	0.71%	1465	1.14%
Гресск Gressk	0.13317	5.57	439.5	0.60%	3698	0.67%	9200	0.90%	19770	0.74%	29940	1.01%	1876	0.88%
Filomena	0.02495	5.5	197.2	0.29%	1010	0.26%	3319	0.31%	17110	0.35%	24550	0.49%	1606	0.22%
duplicate	0.03248	5.6	192.7	0.28%	984.0	0.26%	3306	0.28%	16990	0.31%	24400	0.41%	1586	0.23%
Lombard	0.23097	5.5	151.0	0.26%	735.2	0.26%	2627	0.28%	15620	0.32%	22350	0.44%	1730	0.25%
Old Woman B	0.18319	5.49	44.51	0.27%	248.0	0.26%	849.3	0.29%	12650	0.54%	17560	0.83%	1838	0.30%
Old Woman A	0.19186	5.63	42.90	0.65%	244.2	0.67%	797.3	0.70%	12840	1.31%	17490	1.99%	1753	1.02%
Navajo	0.11729	5.49	26.17	0.30%	156.8	0.25%	503.4	0.25%	11300	0.33%	16010	0.44%	1838	0.25%
Mount Joy	0.18876	5.78	22.15	0.29%	131.7	0.26%	435.5	0.29%	9899	0.73%	14690	1.23%	1880	0.39%
Bilibino	0.20411	5.99	7.272	0.41%	47.45	0.31%	120.8	0.29%	7622	1.56%	9533	2.40%	2069	0.90%
Smithsonian Iron	0.26216	5.55	3.888*	0.41%	28.56	0.29%	58.68	0.27%	5344	1.51%	8354	2.78%	1623	0.95%
Sikhote-Alin	0.16595	6.03	1.429	0.85%	10.64	0.65%	21.13	0.55%	5400	8.56%	3010	6.83%	2330	9.94%
Derrick Peak	0.17345	6.36	1.303	0.87%	10.56	0.67%	16.43	0.57%	4330	11.27%	2560	9.51%	1970	13.74%
Santa Luzia	0.25186	6.04	1.278	0.81%	7.976	0.67%	8.463	0.45%	3400	9.81%	1470	6.43%	2690	18.13%
duplicate	0.16893	6.04	0.8432	1.01%	8.039	0.66%	10.19	0.42%	2020	6.23%	1370	5.81%	1340	10.21%
Sao Juliao de Moreira	0.37235	5.78	0.7154	0.81%	7.285	0.68%	5.730	0.44%	1710	6.12%	1060	5.32%	2080	16.14%

Table 1. The complete compilation of IIAB iron meteorite data (* = obtained from Cook et al. 2004). Ni content obtained from Wasson et al. 2007

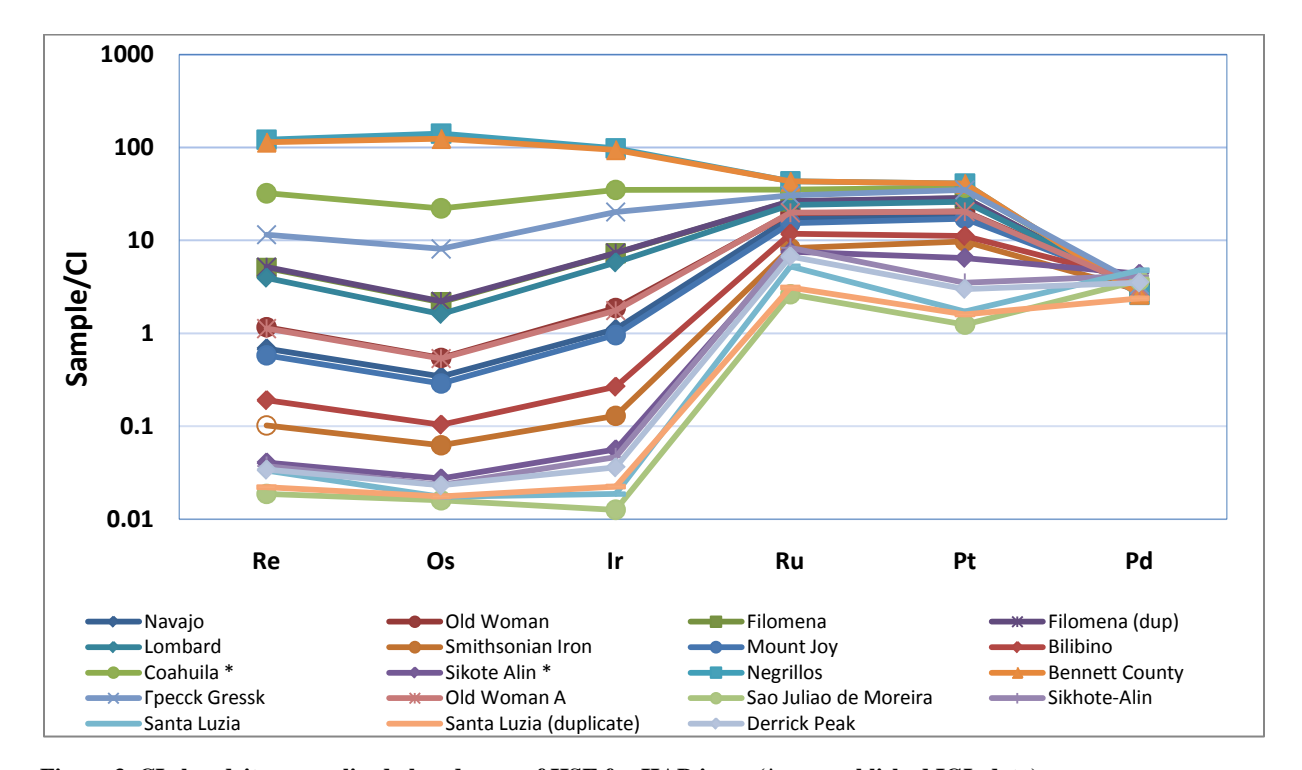
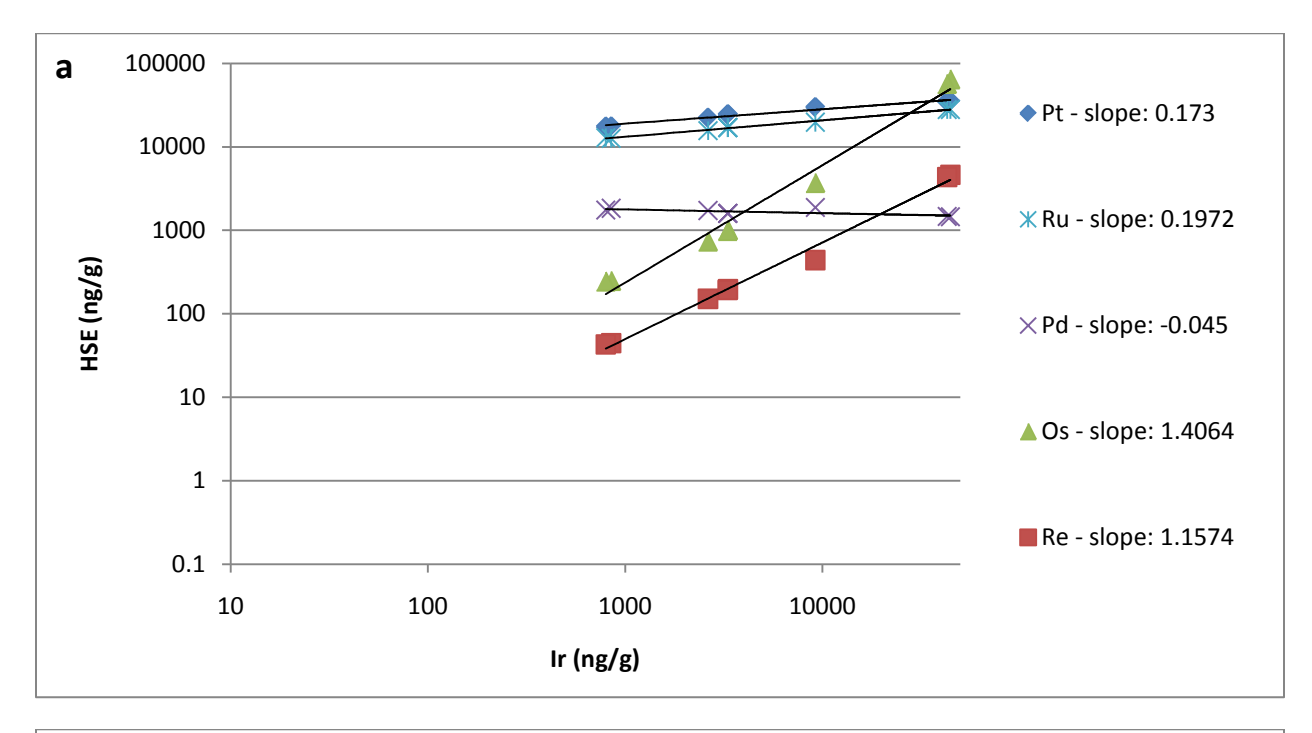


Figure 3. CI chondrite normalized abundances of HSE for IIAB irons (* = unpublished IGL data).

Re, Os, Ru, Pt, and Pd data were plotted versus Ir data for high and low Ir abundant IIAB irons (see figure 4). Old Woman was selected as the midpoint between high and low Ir abundances because the Old Woman meteorite includes both octahedron and hexahedron structures. Doing so, allowed me to obtain two sets of linear regression lines for my data. These isochron regressions allowed me to calculate a required slope for the modeling process.



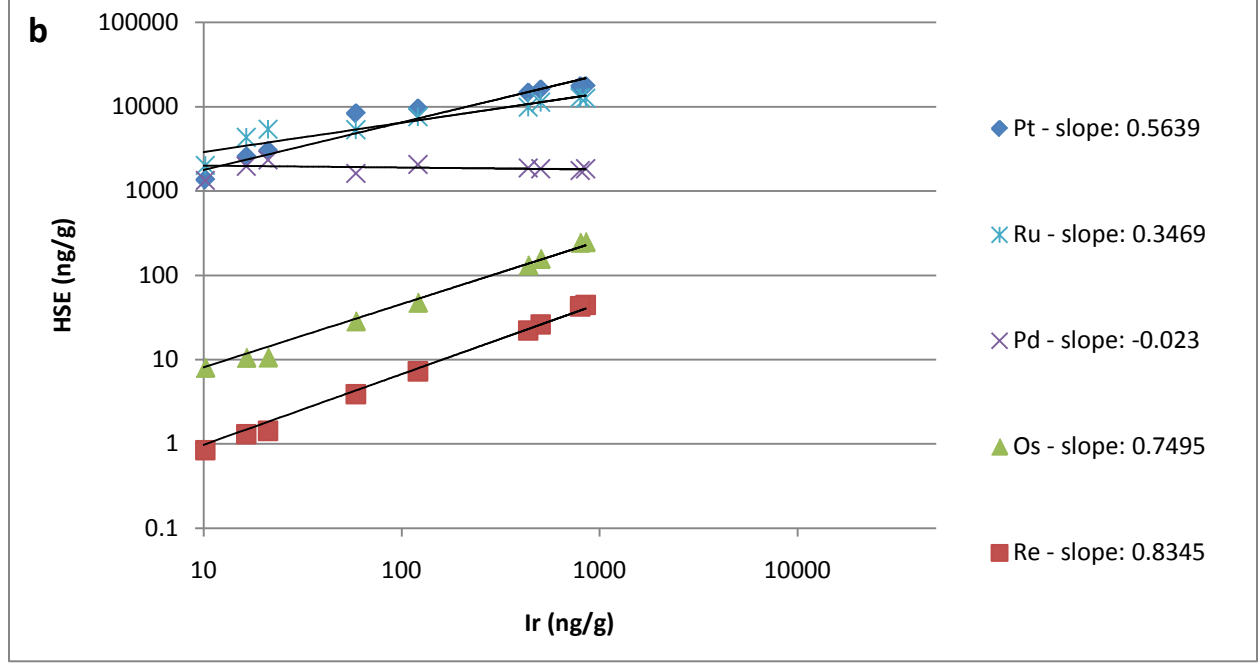


Figure 4. (a-b) Logarithmic plot of Ir versus other HSE concentrations with the steeper slopes (a) representing high Ir samples and shallower slopes (b) representing low Ir samples.

4. DISCUSSION

A crystal-liquid fractionation model was developed to account for the chemical variability in group IIAB iron meteorites. The model is based on the observation that concentrations of Re, Os, Ir, Ru, and Pt decreased during crystallization of the IIAB system. The opposite can be observed with Pd abundances increasing throughout the crystallization process. This means that Pd exhibits incompatible tendencies, while the remaining HSE favor the solid. While these trends have been observed and documented extensively, the determination of precise and accurate *D* values for each HSE during IIAB crystallization for the suite of HSE are problematic. There is also the influence of S and P on the evolution of iron meteorites crystallization. S and P are incompatible, similar to Pd, but impact the *D* values of HSE by raising them as the concentrations of S and P increase. This means that due to relatively high amounts of S and P, the IIAB system is difficult to model.

With extensive research into crystallization systems and a focus on Ir, the D_0 and initial weight percent S for group IIAB irons are known (Chabot et al. 2004). These values are plugged into an equation (see equation 2) in order to determine the how the D values of Ir progress through the crystallization's progress and fit the results to experimentally contrained Ir data. The initial S concentration of 17% was taken from Chabot et al. 2004. This value came from fitting models to Ga, Ge, and Ir versus Au data plots and finding which initial S weight percent allowed the model to work with IIAB irons.

Equation 2. The equation used to calculate the D coefficient for Ir for each increment of fractional crystallization (0.1%). (Chabot et al. 2004)

$$\frac{1}{D_{HSE}} = \frac{\left[\frac{(1 - 2X_S - 3X_P)}{(1 - X_S - 2X_P)}\right]^{\beta}}{D_{0(HSE)}}$$

Taking the D values calculated for Ir and the slopes of the log plots of Ir versus the other HSE, the D values for the remaining HSE are fairly easy to work out. The trick is to use another equation that relates $D_{\rm HSE}$ to $D_{\rm Ir}$ with the help of the slope of correlation (see equation 3). An $D_{\rm HSE}$ values are then be plotted in any multiple configurations and compared to the IIAB abundance data.

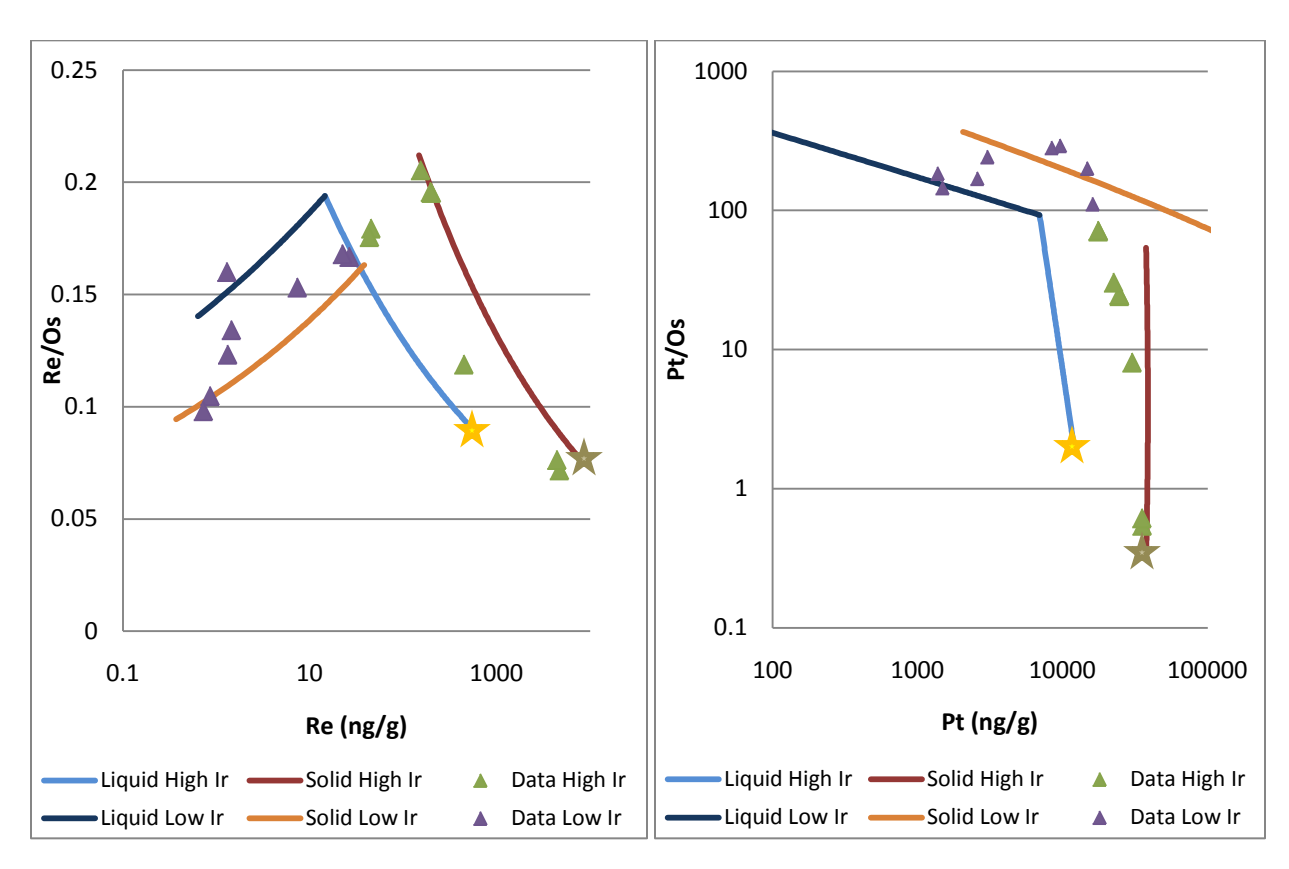
Equation 3. The equation used to calculate the D coefficient for each of the HSE. (Chabot and Jones, 2003)

Slope of correlation =
$$\frac{[D_{HSE}-1]}{[D_{Ir}-1]}$$

The final step after calculating all of these D coefficients, then varying input concentrations, is to calculate liquid and solid tracks that are consistent with the observed evolution of HSE abundances through crystallization.

First, the Re concentrations were plotted against Re/Os ratio for high Ir IIAB irons and the high Ir solid and liquid tracks were added to adjust the initial values for Os and Re. The goal was to find values that placed the solid and liquid tracks on either side of the high Ir data (see figure 5). Then a point just past where Old Woman plotted was selected as the turning point at which the crystallization process began to crystallize the low Ir IIAB irons. The abundance values of the liquid were then used with the low Ir slope values and this generated solid and liquid tracks for the low Ir samples. These new tracks were plotted along with the low Ir samples with nearly all of data points landing within the low Ir tracks. The reason for working with Re and Os first was because the starting Re/Os ratio is constrained by Re/Os chondritic values. The Re-Os system made it possible to determine the break point that would satisfy the Re and Os data which showed two obvious trends. This point was chosen at 26% crystallization with 84% liquid left, and was applied through the rest of the plots where solid and liquid tracks were plotted. Lastly, the starting points were marked with stars for both the liquid and solid tracks.

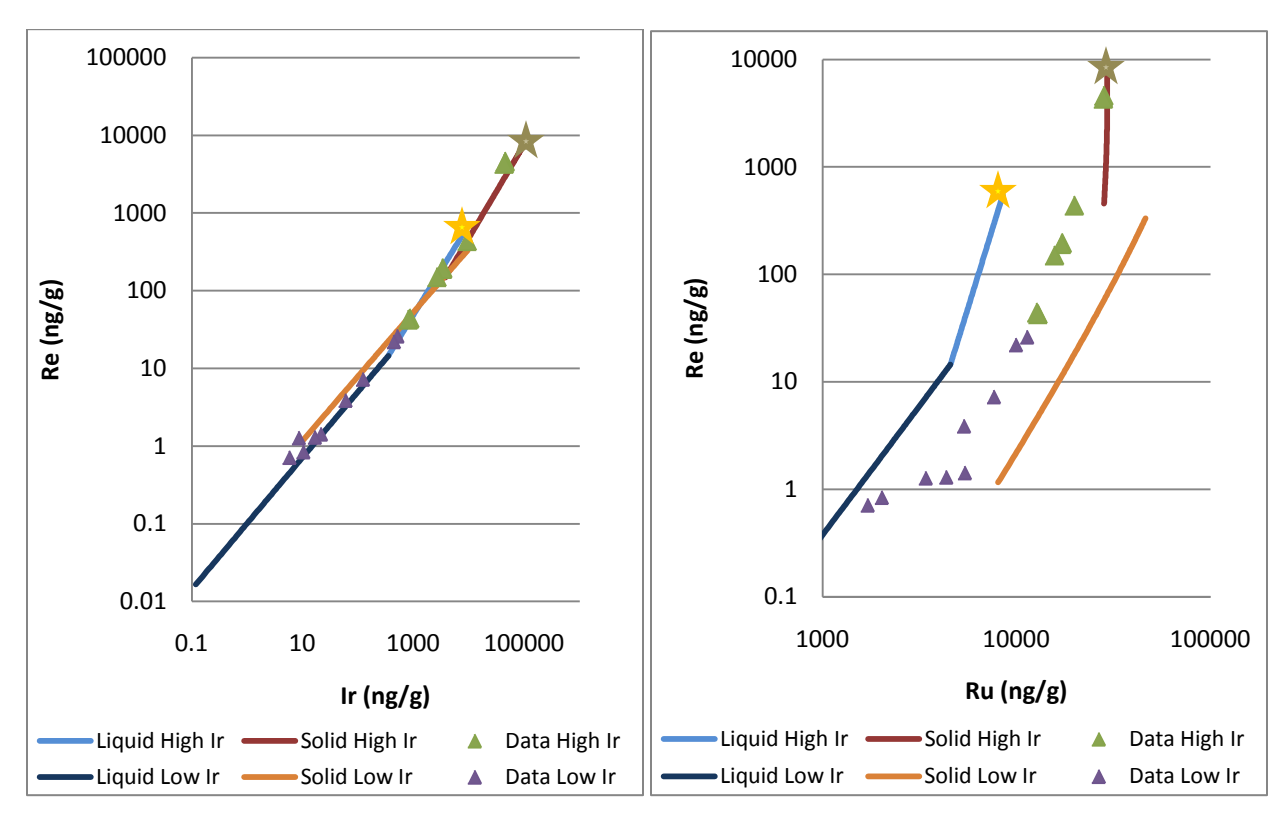
Using the same slope values and break point as the Re and Os, the initial Pt was then tweaked until the majority of the data plotted within the liquid and solid tracks (see figure 6). The reason for following up with Pt next is that it too had Pt/Os ratio that is constrained by chondritic values.



Firgure 5. Log plot of Re/Os ratios versus Re.

Firgure 6. Log-log plot of Pt/Os ratios versus Pt.

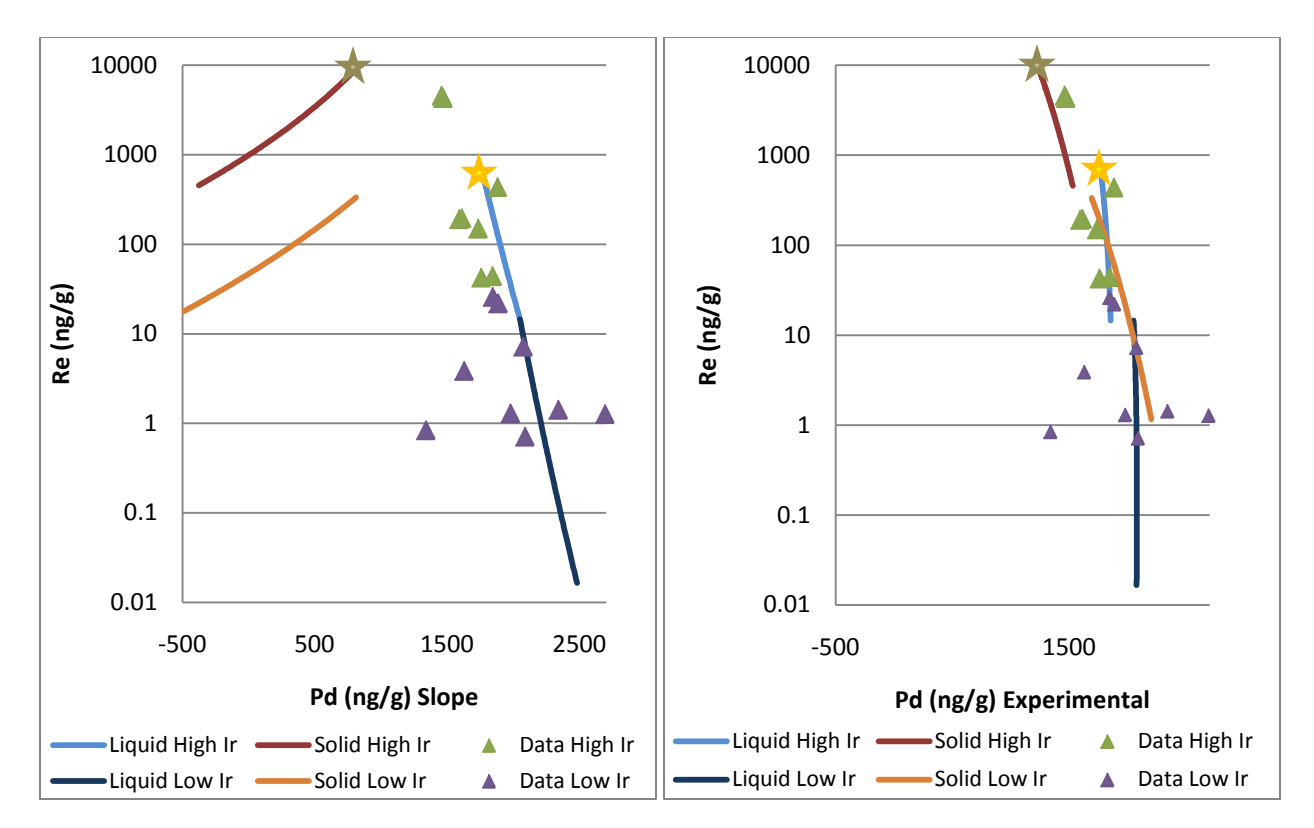
The same process was repeated using starting Re for Ir and Ru (see figures 7 & 8). The Ir and Ru plots both resulted in consistent acceptable fits for the Ir and Ru data.



Firgure 7. Log-log plot of Re versus Ir.

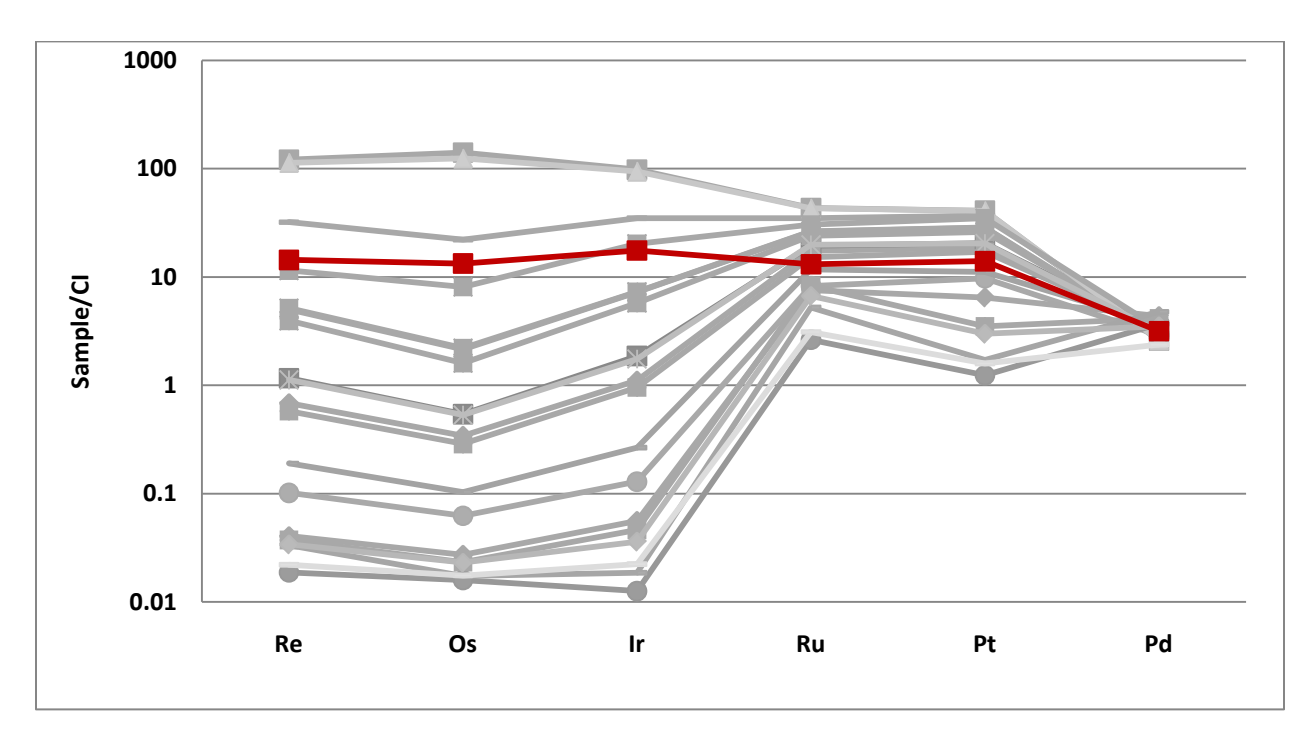
Firgure 8. Log-log plot of Re versus Ru.

Finally, the Pd was modeled using the same slope values and starting concentrations as the other models, yet for Pd there were two alternatives in order to get solid and liquid tracks. One was to use the same slope formula as the previous sets, and the other was to use an experimentally derived method from Chabot and Jones, 2003 (see figures 9 & 10). The Pd part of the model isn't as consistent with my data as predicted in my hypothesis. Once done finding the optimal positions for the tracks for each set, the resulting initial concentrations values represent the calculated starting concentrations of the IIAB system's liquid melt composition for HSE found in group IIAB irons (see figure 11). The fact that Re, Os, Ir, Ru, and Pt are 10 fold more abundant in the core over chondrite values, means that the core must have been on the order of one tenth the size of the parent body. Also, the Pd appears to be depleted in the core resulting in the Pd being found elsewhere in the parent body or a better possibility of my model simply not being able to explain effectively how the Pd crystallized.



Firgure 9. Log plot of Re versus Pd Slope.

Firgure 10. Log plot of Re versus Pd Experiemental.



Firgure 11. Plot of calculated initial concentrations of HSE, normalized to CI chondrites in the IIAB iron's melt. For comparison the values from figure 3 were re-plotted in grey.

5. CONCLUSION

My goal was to as obtain concentration data for a HSE suite of group IIAB iron meteorite samples that span the range of Ni content for this group. Using the methods of solvent extraction, microdistillation, and anion exchange chromatography, I was able to purified samples in order to analyze them on the TIMS and ICP-MS. The concentrations were used to create a viable model for the fractional crystallization of the group IIAB iron meteorites. I hypothesized that previous models for the entire suite of HSE that I am working with would be acceptable but problems would arise due to Pd. Much to my dismay, my prediction was correct and the Pd proved to be too complicated to be explained with my modified model for fractional crystallization. The techniques used were effective and yielded precise concentration measurements but perhaps a more successful model may be possible by building in a function that allows the liquid and solid tracks of crystallization to be deviated without having to start and stop the model. There may also be alternate paths of obtaining starting compositions, and will possibly yield different initial values that may prove to better fit the group IIAB iron meteorite crystallization process.

ACKNOWLEDGMENTS

I have used the following facilities; rock preparation lab, clean lab, TIMS lab, and ICP-MS lab. My advisor, Dr. Walker, assisted me by supplying me with instructions and tools to get the work done. Dr. Igor Puchtel and Dr. James Day provided further help when I required assistance during any period in which Dr. Walker was unavailable. Lastly, my lab comrade Miriam Galenas has been able to assist me with preparation tasks such as cleaning and labeling of sample vessels.

APPENDIX

The University of Maryland Honor Pledge:

"I pledge on my honor that I have not given or received any unauthorized assistance or plagiarized on this assignment."

REFERENCES

- Chabot N. and Jones J. The parameterization of solid metal-liquid metal partitioning of siderophile elements. *Meteoritics & Planetary Science*. October 01, 2003;38(10):1425-1436.
- Chabot N. Sulfur contents of the parental metallic cores of magmatic iron meteorites. *Geochimica et Cosmochimica Acta*. September 01, 2004;68(17):3607-3618.
- Cook D. Pt-Re-Os systematics of group IIAB and IIIAB iron meteorites. *Geochimica et Cosmochimica Acta*. March 01, 2004;68(6):1413-1431.

- Fleet M. Partitioning of trace amounts of highly siderophile elements in the Fe-Ni-S system and their fractionation in nature. *Geochimica et Cosmochimica Acta*. September 1, 1999;63(17):2611-2622.
- Haack H. Asteroid core crystallization by inward dendritic growth. *Journal of Geophysical Research*. September 25, 1992;97(E9):14.
- Jones J. Experimental geochemical investigations of magmatic iron meteorites; modeling complexities. *Meteoritics*. December 01, 1982;17(4):233-233.
- Jones J. Fractional crystallization of iron meteorites; constant versus changing partition coefficients. *Meteoritics*. May 01, 1994;29(3):423-426.
- Krot A. *Classification of meteorites Treatise on geochemistry*. United Kingdom: Elsevier : Oxford, United Kingdom; 2004.
- Luck J. ¹⁸⁷Re-¹⁸⁷Os systematics in meteorites; early chronology of the soler system and age of the Galaxy. *Nature [London]*. January 17, 1980;283(5744):256-259.
- Morgan J. Rhenium-osmium concentration and isotope systematics in group IIAB iron meteorites. *Geochimica et Cosmochimica Acta*. June 01, 1995;59(11):2331-2344.
- Pernicka E. and Wasson J. T. Ru, Re, Os, Pt, and Au in iron meteorites. *Geochimica et Cosmochimicia Acta*. June 1, 1987;51(6):1717-1726.
- Shirey S. B. and Walker R. J. The Re-Os isotope system in cosmochemistry and high-temperature geochemistry. *Annual Review of Earth and Planetary Sciences*. January 1, 1998;26:423-500
- Walker R. J. Modeling fractional crystallization of group IVB iron meteorites. *Geochimica et Cosmochimica Acta* [serial online]. April 15, 2008;72(8):2198-2216.
- Wasson J. Formation of IIAB iron meteorites. *Geochimica et Cosmochimica Acta*. February 01, 2007;71(3):760-781.